Supporting Information

Visible and Near-Infrared Dual-Emission Carbogenic Small Molecular Complex with High RNA Selectivity and Renal Clearance for Nucleolus and Tumor Imaging

Hua He[a], Zhencai Wang[a], Tiantian Cheng[a], Xu Liu[a], Xiaojuan Wang[a], Junying Wang[b], Hao Ren[a], Yawei Sun[a], Yanzhuo, Song[a], Jiang Yang[c], Yongqing Xia[a], Shengjie Wang[a], Xiaodong Zhang[b,] and Fang Huang[a,]**

[a] State Key Laboratory of Heavy Oil Processing and Center for Bioengineering and Biotechnology, China University of Petroleum (East China), Qingdao 266580, China

[b] Department of Physics, School of Science, Tianjin University, Tianjin 300354, China

[c] Environment, Energy and Natural Resources Center, Department of Environmental Science and Engineering, Fudan University, No.220, Handan Road, Shanghai 200433, China

Correspondence should be addressed to F.H. (fhuang@upc.edu.cn)

X.Z. (xiaodongzhang@tju.edu.cn),

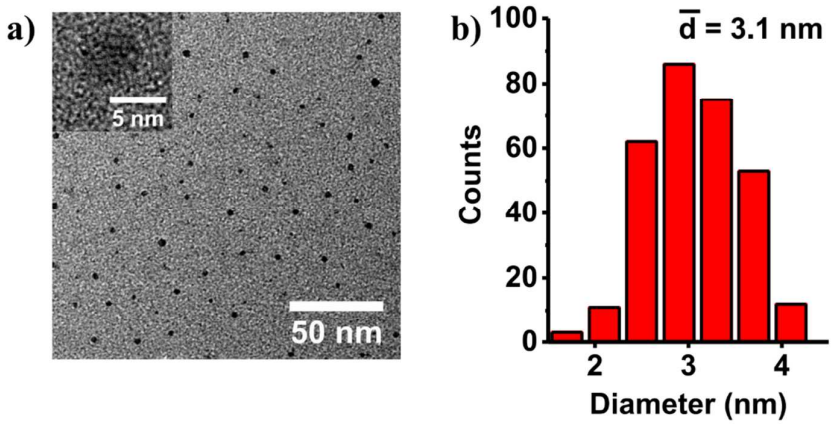

Figure S1. a) TEM and HRTEM (inset) images of carbonized particles; b) Size distribution of particles. The average size is 3.1 ± 0.5 nm.

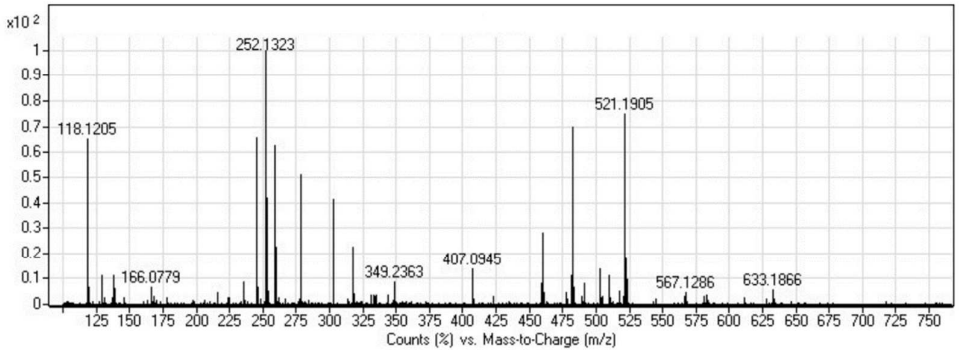

Figure S2. Mass spectra of the products after removing carbonized particles by a dialysis membrane with a 1000-Da molecular weight cutoff.

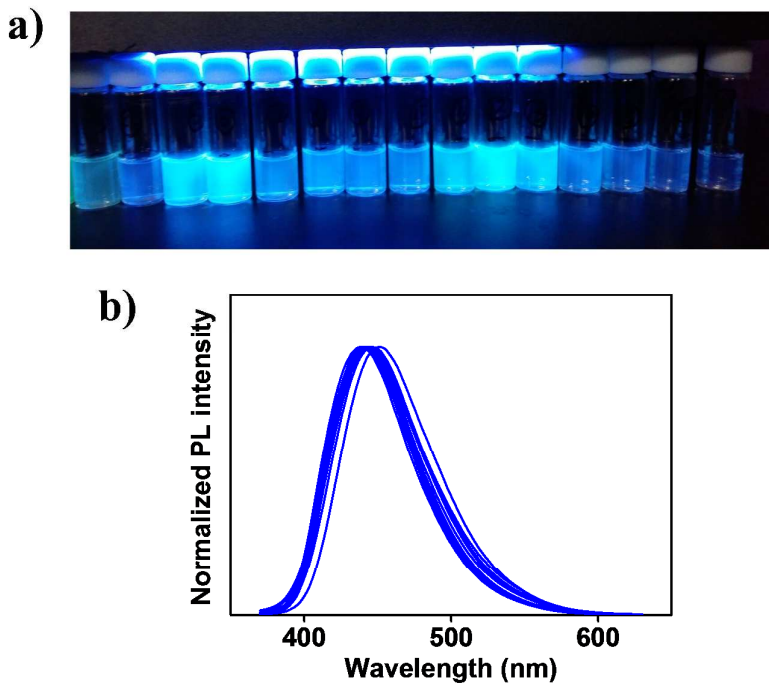

Figure S3. a) Digital photographs of a series of fractions from the as-synthesized products under a 365 nm UV lamp. The products were separated by column chromatography embedded with silica gel using ethyl acetate-methanol (3:1 to 1:3) as eluent; b) Fluorescence spectra of the fractions under 345 nm light excitation.

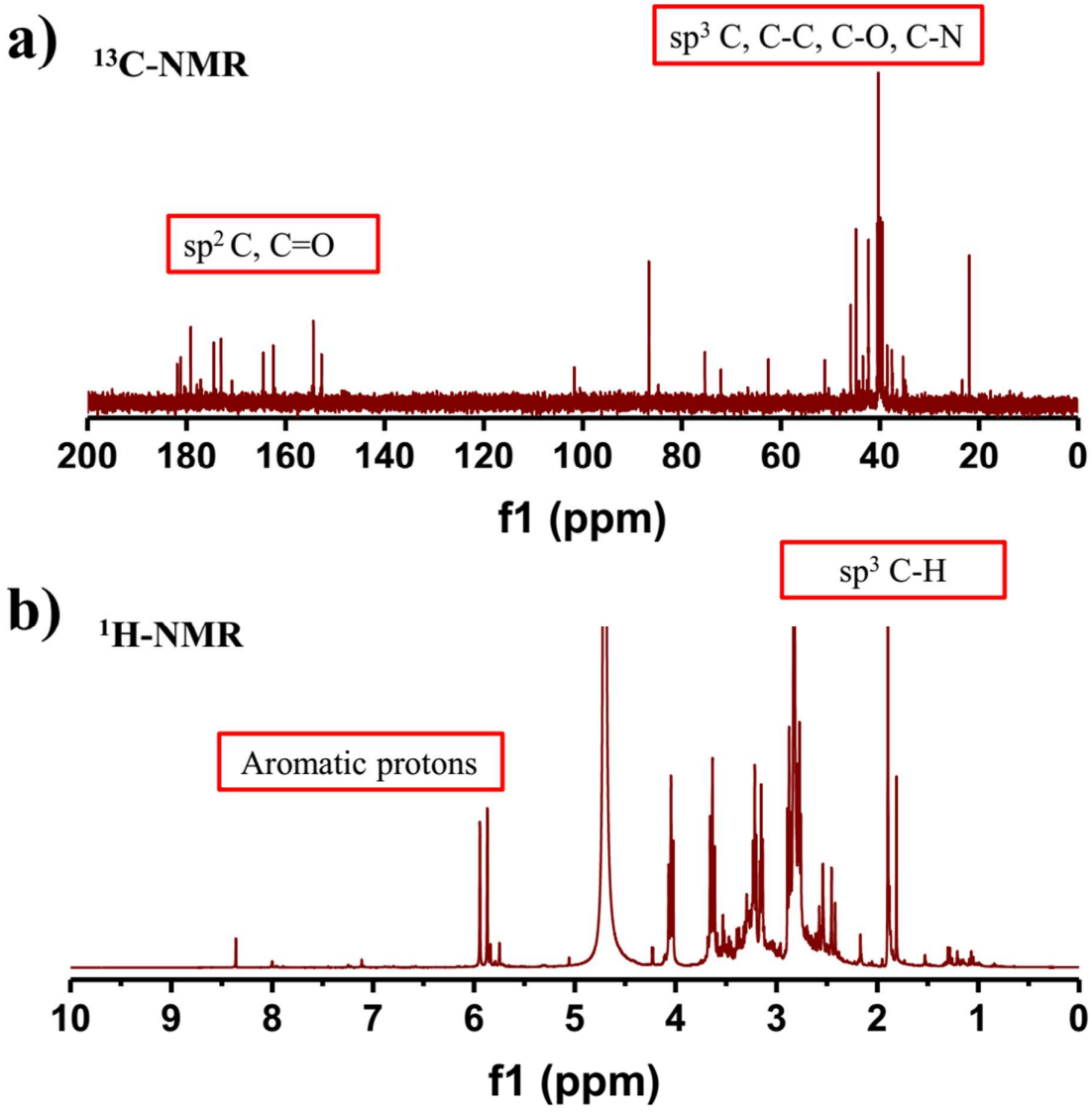

Figure S4. The ^{13}C-NMR (a) and ^{1}H-NMR (b) spectra of SMCs.

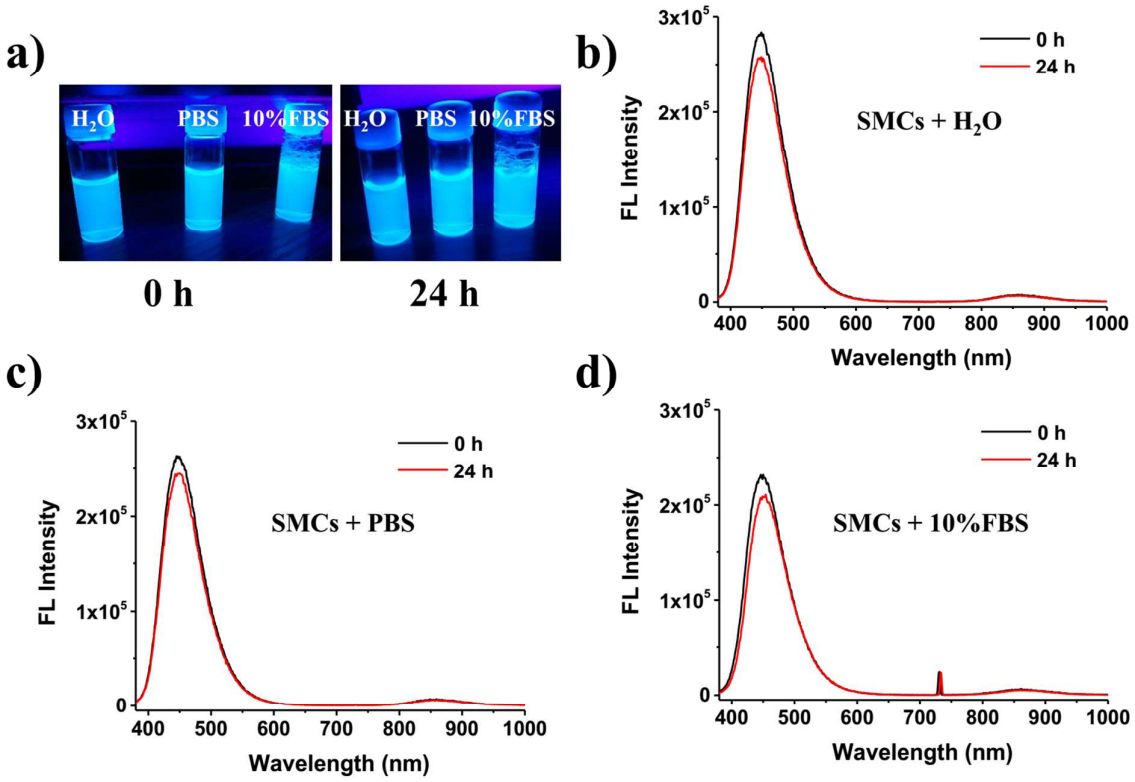

Figure S5. a) Digital photographs of SMCs in H_2O, PBS and 10% FBS solutions under a 365 nm UV lamp; b, c,d) Fluorescence spectra of SMCs before and after 24 h in H_2O, PBS and 10% FBS solutions.

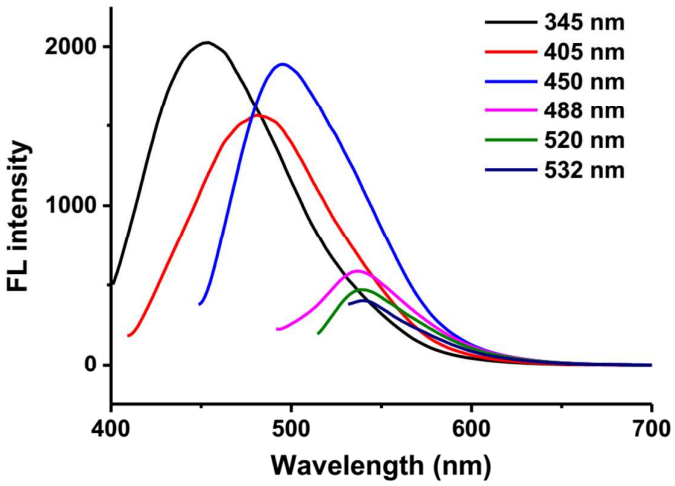

Figure S6. Fluorescence spectra of CDs (obtained from the products above 1000 Da through dialysis as shown in Figure S1) under different excitation wavelengths. The absorbance of CDs at 345 nm = 0.03.

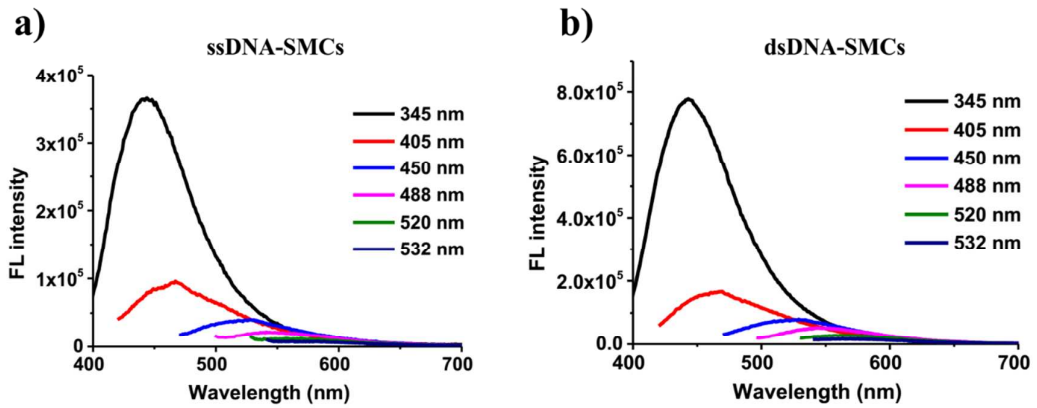

Figure S7. Fluorescence spectra of ssDNA-SMCs (a) and dsDNA-SMCs (b) under different excitation wavelengths. The absorbances at 345 nm for ssDNA- and dsDNA-SMC solutions were measured to be 0.013 and 0.023, respectively.

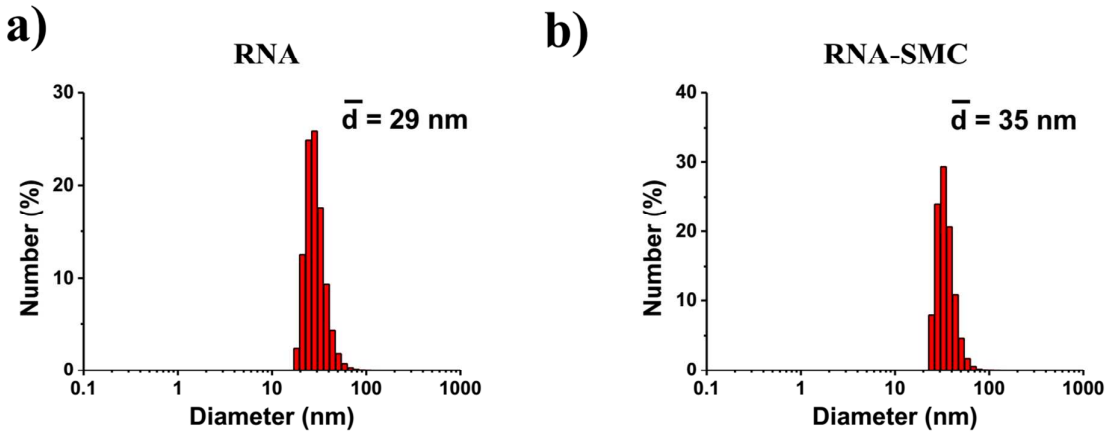

Figure S8. The size distribution of RNA measured by DLS before (a) and after (b) the addition of SMCs.

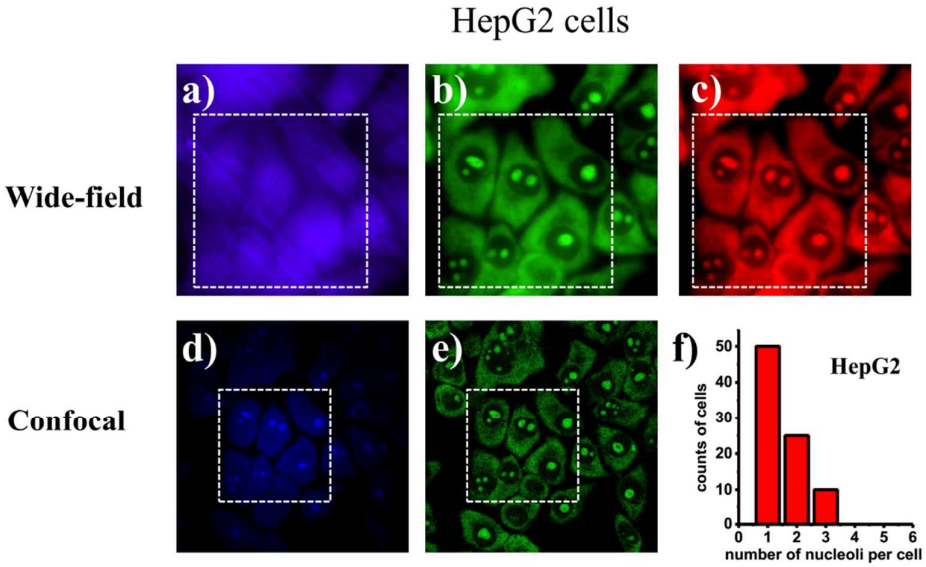

Figure S9. Wide-field fluorescence images of SMC-stained HepG2 cells in blue (a), green (b) and red (c) channels; Confocal fluorescence images of the same field of view as highlighted by white dashed frames under 405 nm (d) and 488 nm (e) laser excitation; f) Frequency distribution of the number of nucleoli per HepG2 cell.

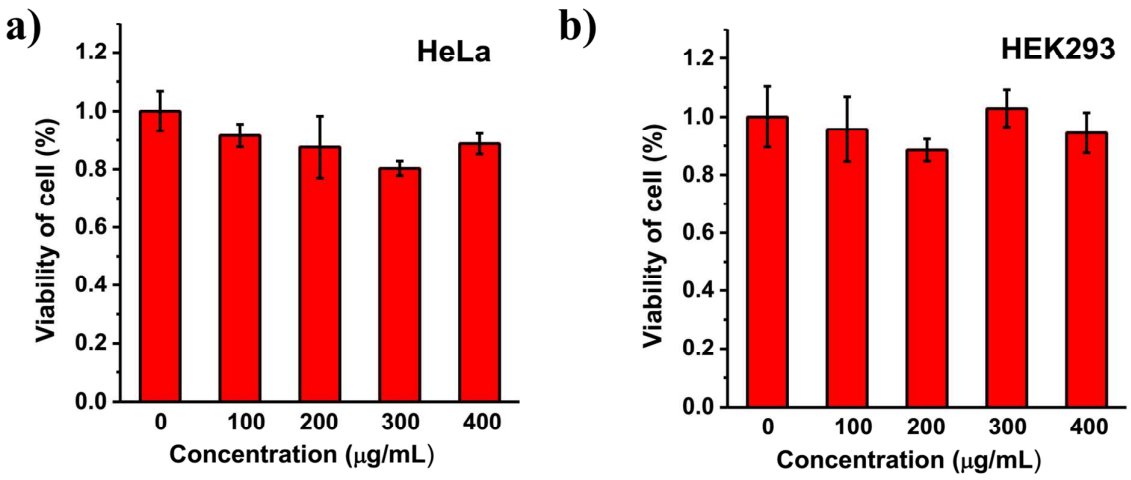

Figure S10. Cytotoxicity of SMCs against HeLa (a) and HEK293 (b) cells by MTT assays, illustrating percentage cell viability at different concentrations of SMCs for 24 h. Non-treated cells is arbitrarily assigned 100% viability. The cells were seeded on 96-well plates at a density of 5×10^3 cells/well in 100 μL medium containing 10% FBS. The plates were then incubated for 24 h at 37 ^{o}C containing 5% CO_2. 100 μL of different concentrations of SMCs in PBS solution were added and the cells were incubated for further 24 h. Wells containing cells without SMCs were used as controls. Subsequently, 20 μL of MTT solution (5 mg/mL) was added to each well and the plates were incubated for further 4 h at 37 ^{o}C. The precipitated formazan was dissolved in 150 μL of DMSO (dimethyl sulfoxide). The absorbance at 590 nm was measured using a microplate autoreader (Multiskan FC, Thermo Scientific). Percent cell survival is expressed as a percent ratio of A590 of cells treated with SMCs over control cells.

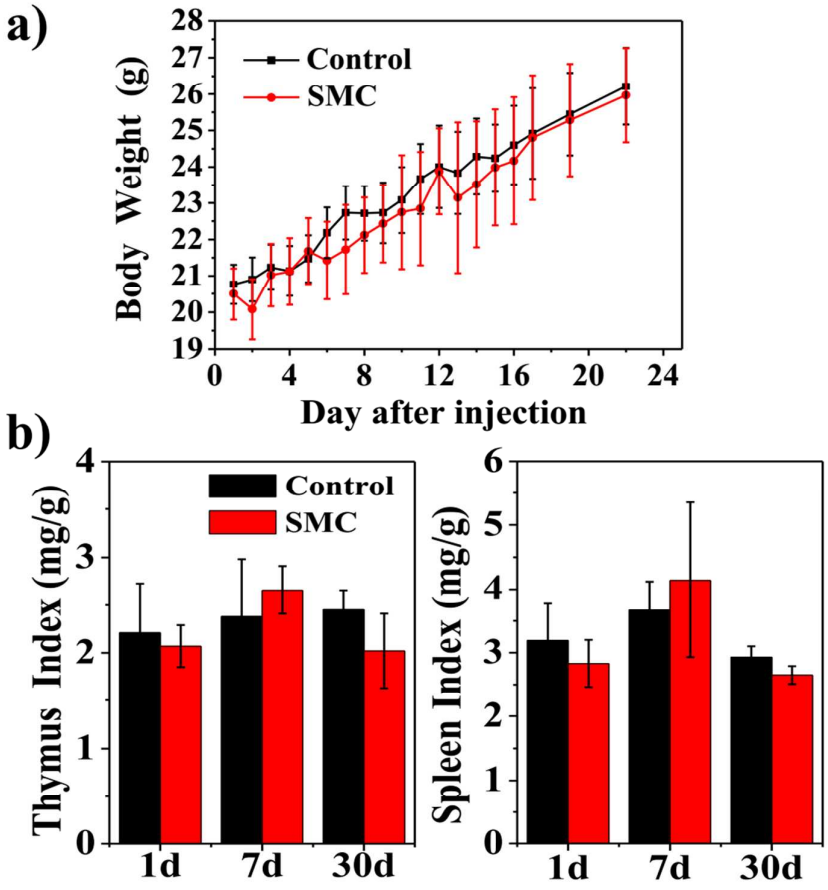

Figure S11. a) Body weight changes for mice treated with SMCs at a dose of 8 mg/mL; b) Spleen and thymus indices of mice after intraperitoneal injection.